REPORT DOCUMENTATION PAGE	Form Approved OMB No. 0704-0188

1. REPORT DATE (DD-MM-YYYY)	2. REPORT TYPE	3. DATES COVERED (From - To)
01-07-2005	Proceeding	

4. TITLE AND SUBTITLE

USING CT TO IMAGE STORM-GENERATED STRATIGRAPHY IN SANDY SEDIMENT OFF FORT WALTON BEACH, FLORIDA, USA

5a. CONTRACT NUMBER

5b. GRANT NUMBER

5c. PROGRAM ELEMENT NUMBER

N602782N

6. AUTHOR(S)

Kevin B. Briggs and Allen H. Reed

5d. PROJECT NUMBER

5e. TASK NUMBER

5f. WORK UNIT NUMBER

7. PERFORMING ORGANIZATION NAME(S) AND ADDRESS(ES)

Naval Research Laboratory
Seafloor Sciences Branch
Stennis Space Center, MS 39529

8. PERFORMING ORGANIZATION REPORT NUMBER

NRL/PP/7430-05-4

9. SPONSORING/MONITORING AGENCY NAME(S) AND ADDRESS(ES)

Office of Naval Research
800 North Quincy Street
Arlington, VA 22217-5660

10. SPONSOR/MONITOR'S ACRONYM(S)

ONR

11. SPONSOR/MONITOR'S REPORT NUMBER(S)

12. DISTRIBUTION/AVAILABILITY STATEMENT

Approved for public release; distribution is unlimited

13. SUPPLEMENTARY NOTES

Proceedings of the International Conference "Underwater Acoustic Measurements: Technologies & Results" Heraklion, Crete, Greece, 28th June - 1st July 2005.

14. ABSTRACT

Abstract: *High-resolution (120-μm) measurements of X-ray attenuation with NRL's HD-500 microfocus Computed Tomography (CT) imager have been accomplished on 5.9-cm-diameter diver-collected cores from an acoustic experiment (SAX04) conducted off Fort Walton Beach, Florida. The purpose of this imagery is ultimately to quantify sediment heterogeneity for modeling acoustic scattering. Cores mainly consisting of medium quartz sand were scanned with X-rays at 114-μm intervals downcore and the images were reconstructed to create a three-dimensional image of sediment density variations from the sediment-water interface to approximately 20 cm sediment depth. The small voxel size (120×120×114 μm) used in the image reconstruction allowed unusually detailed images to be acquired that reveal storm-generated*

15. SUBJECT TERMS

sediments, Computed Tomography, mud, flasers

16. SECURITY CLASSIFICATION OF:			17. LIMITATION OF ABSTRACT	18. NUMBER OF PAGES	19a. NAME OF RESPONSIBLE PERSON
a. REPORT	b. ABSTRACT	c. THIS PAGE			Kevin Briggs
Unclassified	Unclassified	Unclassified	SAR	8	19b. TELEPHONE NUMBER (Include area code) 228-688-5518

Proceedings of the International Conference "Underwater Acoustic Measurements: Technologies & Results"
Heraklion, Crete, Greece, 28th June – 1st July 2005

USING CT TO IMAGE STORM-GENERATED STRATIGRAPHY IN SANDY SEDIMENT OFF FORT WALTON BEACH, FLORIDA, USA

Kevin B. Briggs[a] and Allen H. Reed[a]

[a]Seafloor Sciences Branch, Naval Research Laboratory, Stennis Space Center, MS 39529

Kevin Briggs, Seafloor Sciences Branch, Naval Research Laboratory, Stennis Space Center, MS 39529, FAX: 228-688-5752, kbriggs@nrlssc.navy.mil

Abstract: *High-resolution (120-μm) measurements of X-ray attenuation with NRL's HD-500 microfocus Computed Tomography (CT) imager have been accomplished on 5.9-cm-diameter diver-collected cores from an acoustic experiment (SAX04) conducted off Fort Walton Beach, Florida. The purpose of this imagery is ultimately to quantify sediment heterogeneity for modeling acoustic scattering. Cores mainly consisting of medium quartz sand were scanned with X-rays at 114-μm intervals downcore and the images were reconstructed to create a three-dimensional image of sediment density variations from the sediment-water interface to approximately 20 cm sediment depth. The small voxel size (120×120×114 μm) used in the image reconstruction allowed unusually detailed images to be acquired that reveal storm-generated sedimentary structure that includes mud flasers, laminae from migrating sand ripples and depositional lag layers. Mud flasers are lens-shaped mud inclusions created by the deposition of fine-grained mud onto storm-generated ripples, followed by migration over the mud inclusions of sand ripples mobilized by subsequent storms. The size and shape of the flasers indicate that they were formed from mud immobilized in ripple troughs as the sand ripple crests advanced across the sea floor. Thin, planar, sub-horizontal laminations presumably due to climbing ripples are also evident from the CT images. Above or below sets of planar laminae are comparatively thick layers of homogeneous sand deposition or, infrequently, a coarse, shell-fragment-infused lag layer presumably due to an increase and subsequent decrease in the bottom stress regime.*

CT imaging is largely effective in discriminating among different sediment types and bedding scenarios. Although values of X-ray attenuation of low-density mud and the polycarbonate plastic core liner are very similar, we are able to image the mud through filtering the X-ray beam, amplifying the image intensity, and masking everything outside the region of interest (ROI). Density variations, mud-filled burrows, laminae, and individual sand grains are successfully imaged with the CT system.

Keywords: *sediments, Computed Tomography, mud, flasers*

1. INTRODUCTION

Sedimentary structure is generated by fluid that transports individual grains and ultimately deposits them elsewhere, usually organized into bedforms. The shape, scale, thickness, and grain size of the bedforms depend on the magnitude of the fluid stress on the seafloor. Occasionally, more than one type of bedform is found within sediments, suggesting that the fluid stress was variable over time. Structural components of bedforms, i.e., bedding, consists of layers, laminae, or lenses. The interpretation of bedding in surficial sediments is valuable because it can help define the scale of sediment heterogeneity, define the sedimentary regime, and assist in quantifying estimates of the current strength in modern and ancient sediments [1].

Traditional stratigraphic analysis entails manually splitting the cores to delineate vertical fluctuations of bedding. This methodology provides only a two-dimensional image, with no documentation of bedding slopes without destruction of the sample and/or multiple cores. Investigating stratigraphy of the near-surface sediments has been accomplished with the REMOTS camera, which provides a two-dimensional image from penetration of a wedge-shaped window 10-30 cm into the sediment. Because heterogeneities within the sediment fabric are manifested as variations in bulk density, which is a function of sediment porosity, electrical resistivity imaging of the sediment has been used to determine the bedding characteristics where ionic conduction in the pore fluid is the dominant electrical conduction process [2]. Briggs et al. [3] showed results similar to two-dimensional core slabbing and REMOTS images for mud using resistivity imaging.

The sediment patterns of bedding also are indicated by the fluctuations in sediment density to X-rays, often depicted in X-radiographs of sediment cores [4-6]. Features prominent in X-radiographs are density discontinuities created by episodic bedding as well as interruption of bedding by bioturbation by benthic organisms within the sediment [7]. Use of an electrical resistivity array to image sediment heterogeneity in sands has yielded three-dimensional results with resolution that varies with depth [8]. The recent application of Computed Tomography (CT) imaging to sedimentology has enabled researchers to examine sediment heterogeneity at a much finer resolution than the aforementioned procedures [9, 10]. CT creates volumetric images of three-dimensional media by creating X-rays, passing the X-rays through the media, collecting X-ray attenuation data, converting the attenuation data to images. Ultimately the data is converted to three-dimensional images. Such detailed, volumetric images of sediment bedding should facilitate examination of layer contacts as well as bedding geometry.

Besides offering information on the sedimentary history of the sea floor, statistical quantification of sediment density heterogeneity is of great value in modeling acoustic scattering from the sediment volume. From characterization of fluctuations in sediment density and sound velocity (the two components of acoustic impedance), significant parameters employed in predicting sediment volume scattering of sound energy can be estimated. The magnitude of the fluctuations in sediment impedance determines the acoustic scattering intensity whereas the spatial distribution of the sediment fluctuations determines the frequency and grazing angle dependence of the scattering [11].

2. METHODS AND RESULTS

Divers collected 58 cores from a 1-km^2 area around the R/V Seward Johnson which was anchored in a four-point mooring off the coast from Fort Walton Beach, Florida, USA as part of

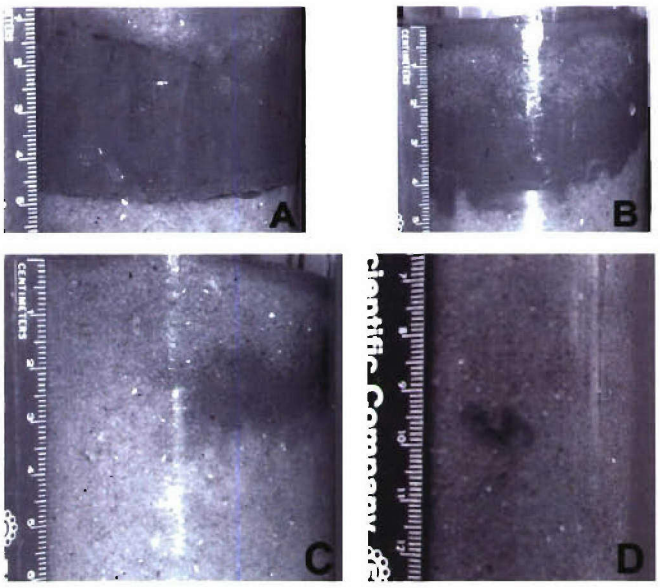

Fig. 2: Types of mud inclusions in SAX04 cores: (A) continuous layer, (B) layer with sand lens, (C) flaser, and (D) isolated mud clast. Photos A, B, and C courtesy of D. Tang.

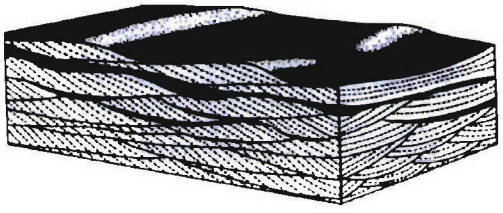

Fig. 3: Flaser bedding, showing draping of mud (dark) over sand ripples (light). Figure used with permission from AAAS [12].

Mud inclusions in the cores were exemplified by four types of features: continuous layers, mud layers with sand lenses, flasers, and isolated mud clasts (Fig. 2).

3. VISUAL INTERPRETATION OF RESULTS

The four types of inclusions in Figure 2 are actually different manifestations of a process in which fine-grained sediment settles onto sand ripples and is preserved upon mobilization of the coarser-grained sediment. Prior to the collection of diver cores (16 September), Hurricane Ivan came ashore 100 km to the west of the experiment site. The seas accompanying the category 4 hurricane, presumably 10-12 m high, breached the sub-aerial dunes of the barrier island north of the site and inundated the lagoon as well as the narrow barrier island. Upon retreat of the seas and storm surge a significant amount of lagoonal mud was transported onto the shelf, where it formed a continuous-to-quasi-continuous layer of mud (Figs. 2A, 3). Following the draping of mud on the surface of the sand, wind-wave activity from Hurricane Jeanne to the east (26 September), and, later, Tropical Storm

Matthew to the west (8 October) mobilized sediment. Some of the mud layer was resuspended and sand from the crests was transported onto the remaining mud layer; settling of the suspended mud resulted in the formation of sand lenses within the mud drape (Fig. 2B). Lens-shaped mud inclusions within the sand sediment are called flasers and are created when the mud that settled into the troughs of ripples is covered by migrating sand ripples, such that the mud is included in the bottom sediment and protected from resuspension by bottom currents (Figs. 2C, 3). The lens-shaped character of the flaser is a result of the deposit assuming the shape of the trough and/or flanks of the sand ripples. Eventually, storm events will break up the surface mud layer into small clasts, which will subsequently be isolated and buried by migrating sand (Fig. 2D).

Thin, even, parallel sand laminae in cores were found below the top 7-8 cm of sediment. In most of these cores, the top 7-8 cm was a homogeneous sediment layer devoid of apparent bedding above the laminae (Fig. 1). Below this layer, laminae existed to depths no greater than 20 cm in the cores. Tilt angles of the laminae varied from 0° to 20° to the horizontal, with the most common angle being 20°. Most laminae were upward-curving, suggesting that these laminations are wave-ripple bedding resulting from storm waves generated during Hurricane Ivan [1]. Also, the presence of parallel, tilted, in-phase climbing-ripple bedding indicates that the ripples that generated the bedding were formed during high suspended sediment load [14]. The wave-ripple bedding was almost certainly generated by the erosion and deposition of the seabed during Hurricane Ivan. Meteorological data from the National Data Buoy Center for the station located 186 km SSE from the study area indicate a peak wave height of 6.9 m and a dominant wave period of 14.3 s. Waves of this magnitude, or larger, likely impinged on the study site: the radial distance from the location where Ivan made landfall to the study site is 24 km less than the radial distance to the data buoy. Given the wave characteristics and the water depth at the study area (16.5 m), the maximum water velocity at the bottom is estimated to be 2.4 m/s and the maximum bottom stress is estimated to be 16.6 Pa [14]. Whereas the critical bed stress for the medium sand at the study area is only 0.216 Pa, the sea floor would have experienced sheet flow with 84% of the sediment transport in the suspended load above the bed [15]. Thus, it is conceivable that the sea floor was eroded down to the base of the ripple bedding at the peak of the wave activity and that the climbing ripples were generated subsequently during the waning of the wave activity.

4. CT IMAGERY

Computed Tomography (CT) imagery is fundamentally the three-dimensional geometric reconstruction of X-ray attenuation data. Materials imaged with CT effectively show internal structure if the components exhibit different X-ray attenuation values. To effectively use the ability of the X-ray source to discriminate among the various levels of attenuation present in the core samples, we limit the X-ray energy level so as to tailor the range to the material. Furthermore, to restrict the information to what is inside the core liner, we fill the field of view with the core during scanning and reconstruct images that contain a Region of Interest (ROI) thus maximizing resolution for each image. As it happens, the polycarbonate core liner containing the sediment samples has attenuation values almost identical to the mud. Because we can set the threshold for the images to exclude attenuation values less than or equal to that of the core liner, reconstructed core images may exclude any data from the mud, and only image inclusions within the mud that have attenuation values higher than the mud. Once this imagery is collected the attenuation values can be thresholded to depict a three-dimensional reconstruction of the space in the core occupied by mud, excluding the space occupied by sand lenses (Fig. 4).

The appearance of the mud-sand interface in the CT image provides information on the processes that created the sediment feature. The uneven texture of the mud surface and the shape of the mud interface, in Figure 4, indicate that the sand has filled a fractured mud surface. That is, some of the mud deposit was likely torn away, probably in clasts, before the sand filled in the depression and preserved the fracture surfaces. Also apparent in the image is evidence of pull-down of sand and mud by the core liner to deeper parts of the core when the core was collected.

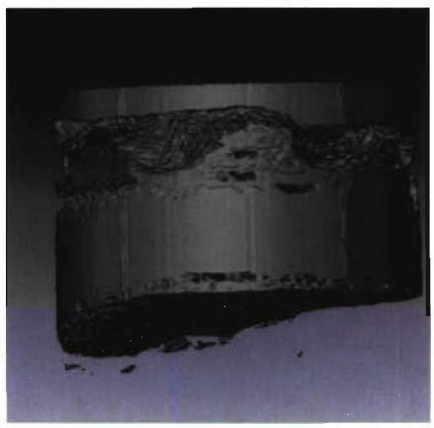

Fig. 4: Three-dimensional reconstruction of CT image of the top 55 mm of core FWB9-2 (Fig. 2B). A sand lens occupies the missing space within the mud layer.

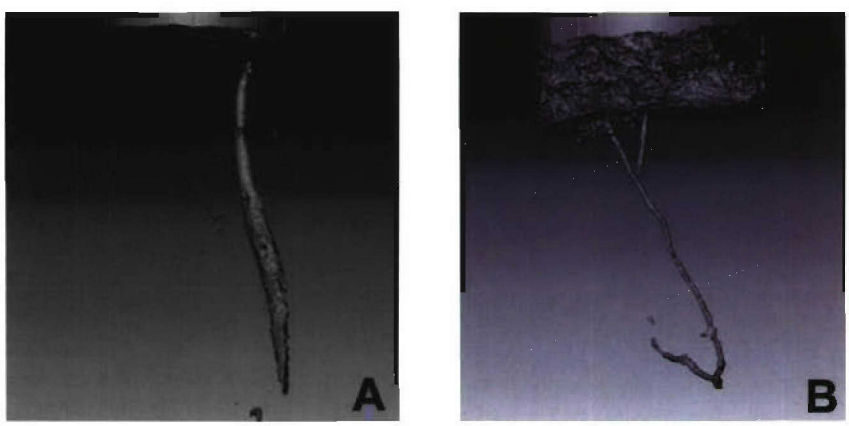

Fig. 5: Three-dimensional reconstruction of CT images of mud-filled burrows: (A) the top 110 mm of core FWB4-1 and (B) top 95 mm of FWB5-2.

Another mechanism by which mud is buried within sand sediments is by infilling of animal burrows with surface mud. Often the mud inundating the burrow will kill or evict the inhabitant, resulting in isolation of the mud-filled burrow as sand covers the inactive opening at the surface. Burrows with relatively large diameters are prone to this mud-filling process (Fig. 5A). Smaller diameter burrows can infill by the feeding or irrigation activities of the burrow inhabitant, producing narrow, meandering mud tubes leading up into the deposited mud at the sediment surface (Fig. 5B).

Although the appearance of mud layers in sand sediment is visually dramatic in CT imagery, discerning laminae created by climbing wave ripples is not easily rendered by reconstruction of X-ray attenuation data. Due to the subtle and graded differences in sediment density present in sand ripple laminations (especially compared to the density difference between mud and sand), sediment structure is imaged less well by CT than optical methods. By binning the small X-ray attenuation differences and assigning a different color or shading to the binned values, CT images can illustrate the inclined laminae apparent in Figure 1 (Fig. 6). The subtle differences that indicate the presence of laminae are due to different packing arrangements of the sand grains. High-resolution scans of resin-impregnated cores containing climbing-ripple laminae suggest that there is a grain size difference associated with the banded appearance, *i.e.*, an alternation of finer and coarser grain size corresponding to successive laminae (Fig. 6). These images demonstrate that fine-scale fluctuations of physical properties can be measured with CT imagery.

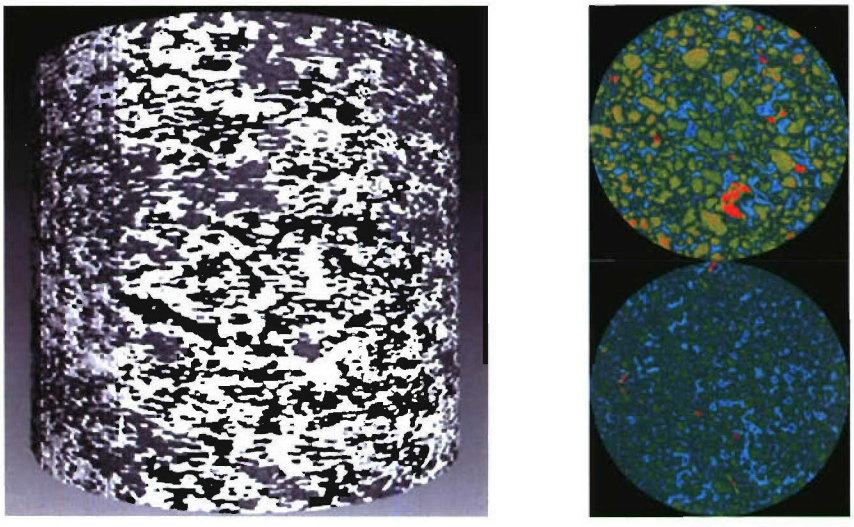

Fig. 6: Left: Three-dimensional reconstruction of 90-130 mm sediment depth of core FWB11-2, showing climbing ripple laminae as subtle periodic banding due to slight bulk density differences created by packing arrangements. Right: Successive 11.16-mm-diameter "slices" (horizontal images) at 5-mm intervals from core FWB19-2 in the 95-to-100-mm-interval displaying alternating coarser- and finer-grained laminae. Small, very dark (fuchsia in false color scheme) grains are the rutile particles; large, dark (red in false color scheme) grains are calcareous shell fragments. Dark borders around light-colored grains are a result of averaging densities of grain and surrounding water.

Also present within CT images of the cores are numerous "streaming" artifacts emanating from relatively high-density particles. These particles are about 50-250 μm in diameter and are distributed throughout the sand. The streaming effect is due to the large amount of X-ray scattering from metals and presumably these particles are rutile (TiO_2) or rutilated quartz, as sands from the West Florida Sand Sheet are known to contain this heavy mineral [16].

5. ACKNOWLEDGEMENTS

We thank R. Ray, C. Vaughan, D. Lott, M. Richardson, K. Williams, T. Hefner, E. Boget, P. Aguilar, E. Kloess, and J. Piper for diving support during SAX04. We also thank the captains and crew of the R/V Pelican, R/V Seward Johnson, and M/V Aquanaut for ship support. Thanks to N. Plant, J. Calantoni, and T. Holland for helpful discussions on sediment transport. This work was supported by the Office of Naval Research, Ocean Acoustics Program and by the Naval Research Laboratory, program element N602782N. Contribution no. NRL/PP/7430-05-4.

REFERENCES

[1] **H.-E. Reineck** and **I. B. Singh**, *Depositional Sedimentary Environments*, Springer-Verlag, New York, 549 pp, 1980.

[2] **P. D. Jackson, D. Taylor Smith** and **P.N. Stanford**, Resistivity-porosity-particle shape relationships for marine sands, *Geophysics,* 43, pp.1250-1268, 1978.

[3] **K. B. Briggs, P. D. Jackson, R. J. Holyer, R. C. Flint, J. C. Sandidge,** and **D. K. Young**, Two-dimensional variability in porosity, density, and electrical resistivity of Eckernförde Bay sediment, *Contin. Shelf Res.*, 18(14/15), pp.1939-1964, 1998.

[4] **J. D. Howard**, X-ray radiography for examination of burrowing in sediments by marine invertebrate organisms, *Sedimentology*, 11, pp.249-258, 1968.

[5] **D. C. Rhoads, R. C. Aller,** and **M. B. Goldhaber**, The influence of colonizing benthos on physical properties and chemical diagenesis of the estuarine seafloor, In *Ecology of Marine Benthos*, University of South Carolina, Columbia, SC, B. C. Coull, Ed., pp.113-138, 1977.

[6] **P. D. Jackson, K. B. Briggs,** and **R. C. Flint**, Evaluation of sediment heterogeneity using microresistivity imaging and X-radiography, *Geo-Mar. Lett.*, 16(3), pp.219-225, 1996.

[7] **M. D. Richardson, D. K. Young,** and **K. B. Briggs**, Effects of hydrodynamic and biological processes on sediment geoacoustic properties in Long-Island Sound, USA, *Mar. Geol.*, 52(3/4), pp.201-226, 1983.

[8] **P. D. Jackson**, personal communication.

[9] **T. H. Orsi, C. M. Edwards,** and **A. L. Anderson**, X-ray computed tomography: A non-destructive method for quantitative analysis of sediment cores, *J. Sediment. Res.*, A64, pp.690-693, 1994.

[10] **R. A. Ketcham** and **W. D. Carlson**, Acquisition, optimization and interpretation of X-ray computed tomographic imagery: Applications to the geosciences, *Comput. Geosci.*, 27, pp.381-400, 2001.

[11] **K. B. Briggs**, *High-frequency acoustic scattering from sediment interface roughness and volume inhomogeneities*, Ph.D. dissertation, University of Miami, 143 pp., 1994.

[12] **H.-E. Reineck**, Layered sediments of tidal flats, beaches and shelf bottoms of the North Sea, *Estuaries*, G. H. Lauff, Ed., AAAS, Publ. 83, pp.191-206, 1967.

[13] **A. V. Jopling** and **R. G. Walker**, Morphology and origin of ripple-drift cross lamination, with examples from the Pleistocene of Massachusetts, *J. Sediment. Petrol.*, 38, pp.971-984, 1968.

[14] **U.S. Army Corps of Engineers**, *Shore Protection Manual, vol. I, 4th Ed.*, Dept. Army, Wash., D.C., 608 pp., 1984.

[15] **R. L. Soulsby**, *Dynamics of marine sands*, Thomas Telford, London, 249 pp., 1997.

[16] **T.H. van Andel** and **D. H. Poole,** Sources of Holocene sediments in the northern Gulf of Mexico, *J. Sediment. Petrol.*, 30(1), pp 91-122, 1960.